Original Article

Direct exposure of non-equilibrium atmospheric pressure plasma confers simultaneous oxidative and ultraviolet modifications in biomolecules

Yasumasa Okazaki,[1] Yue Wang,[1] Hiromasa Tanaka,[2,3] Masaaki Mizuno,[3] Kae Nakamura,[4] Hiroaki Kajiyama,[4] Hiroyuki Kano,[5] Koji Uchida,[6] Fumitaka Kikkawa,[4] Masaru Hori[2] and Shinya Toyokuni[1,*]

[1]Department of Pathology and Biological Responses and [4]Department of Obstetrics and Gynecology, Nagoya University Graduate School of Medicine, 65 Tsurumai-cho, Showa-ku, Nagoya 466-8550, Japan
[2]Plasma Nanotechnology Research Center and [6]Laboratory of Food and Biodyamics, Graduate School of Bioagricultural Sciences, Nagoya University, Furo-cho, Chikusa-ku, Nagoya 464-8601, Japan
[3]Center for Advanced Medicine and Clinical Research, Nagoya University Hospital, 65 Tsurumai-cho, Showa-ku, Nagoya 466-8550, Japan
[5]NU Eco-Engineering Co. Ltd, 2-3-8 Kurozasaizumi, Miyoshi-shi, Nagoya 470-0232, Japan

(Received 1 March, 2014; Accepted 9 June, 2014; Published online 9 September, 2014)

Thermal plasmas and lasers are used in medicine to cut and ablate tissues and for coagulation. Non-equilibrium atmospheric pressure plasma (NEAPP) is a recently developed, non-thermal technique with possible biomedical applications. Although NEAPP reportedly generates reactive oxygen/nitrogen species, electrons, positive ions, and ultraviolet radiation, little research has been done into the use of this technique for conventional free radical biology. Recently, we developed a NEAPP device with high electron density. Electron spin resonance spin-trapping revealed •OH as a major product. To obtain evidence of NEAPP-induced oxidative modifications in biomolecules and standardize them, we evaluated lipid peroxidation and DNA modifications in various *in vitro* and *ex vivo* experiments. Conjugated dienes increased after exposure to linoleic and α-linolenic acids. An increase in 2-thiobarbituric acid-reactive substances was also observed after exposure to phosphatidylcholine, liposomes or liver homogenate. Direct exposure to rat liver in saline produced immunohistochemical evidence of 4-hydroxy-2-nonenal- and acrolein-modified proteins. Exposure to plasmid DNA induced dose-dependent single/double strand breaks and increased the amounts of 8-hydroxy-2'-deoxyguanosine and cyclobutane pyrimidine dimers. These results indicate that oxidative biomolecular damage by NEAPP is dose-dependent and thus can be controlled in a site-specific manner. Simultaneous oxidative and UV-specific DNA damage may be useful in cancer treatment.

***Key Words*:** **non-equilibrium atmospheric pressure plasma, electron spin resonance spin-trapping, 8-OHdG, HNE-modified protein, UV**

The development of nano-scale material processing has greatly contributed to the advancement of high-technology industry. Thermal plasmas and lasers have also been used in medicine to cut and ablate tissues and to stimulate coagulation. Recently, the non-thermal technique of non-equilibrium atmospheric pressure plasma (NEAPP) has been developed.[1] In the physical sciences, plasma is defined as the fourth state of matter (after solid, liquid and gas); plasma is composed of electrons, various ions, ultraviolet (UV) radiation, and reactive oxygen/nitrogen species (ROS/RNS), including ozone, hydrogen peroxide, singlet oxygen, superoxide, hydroxyl radical and nitric oxide. These molecules have potential novel applications and have attracted the attention of medical investigators. From an early stage, studies on the biological properties of plasma have suggested that plasma may have disinfectant properties.[1–4] Recently, several reports have provided evidence that NEAPP exposure affects mitochondria, antioxidant enzymes, cell signaling and the transcriptome of mammalian cells and tissues through ROS.[4–7]

Preclinical studies are also in progress worldwide regarding the potential applications of NEAPP to cancer treatment. The same dose of NEAPP selectively induced cellular damage and caused apoptosis in malignant cells but not in non-tumor cells.[8–11] These results may create a paradigm shift in cancer therapy for currently intractable conditions such as peritoneal carcinomatosis. Reportedly, a quiescent state is required to maintain the stemness of hematopoietic stem cells.[12] Stem cells in cancer, which are the sources of autonomously proliferating cells, cause relapses, chemotherapy-resistance and metastases. Driving cancer stem cells out of the quiescent state into the proliferative period of the cell cycle has been proposed as a potentially curative cancer treatment. A variant form of CD44, a marker of cancer stem cells, transports cysteine and increases the reduced form of intracellular glutathione (GSH),[13] suggesting the importance of ROS regulation in cancer stem cells and the possibility of the topical use of NEAPP to disrupt cancer cells[14] with a mixture of physical agents.

To standardize the measurement of the biological effects of NEAPP, we employed a NEAPP device that generates approximately 100-fold higher density electrons than conventional atmospheric pressure plasma. Using this device, both fungal disinfection and the selective killing of brain (glioblastoma) and ovarian (adenocarcinoma) cancer cells have been reported, indicating that the plasma treatment has biologic activity.[2,9,10] In the present study, we used several different *in vitro* and *ex vivo* systems to evaluate the effects of direct NEAPP exposure, using established techniques in free radical biology. We found that direct exposure of NEAPP simultaneously induces time-dependent oxidative and UV-induced damage of biomolecules.

Materials and Methods

Chemicals. The 2-thiobarbituric acid-reactive substances (TBARS) assay kit was purchased from Oxford Biomedical Research (Oxford, MI). Linoleic acid, α-linolenic acid, phosphatidylcholine (PC) from egg yolk, 5,5'-dithio-*bis*-2-nitrobenzoic acid (DTNB), glutathione reduced form (GSH), and ECOS Competent *E. coli* JM109 were obtained Wako (Osaka, Japan).

*To whom correspondence should be addressed.
E-mail: toyokuni@med.nagoya-u.ac.jp

doi: 10.3164/jcbn.14-40

Vitamin E-stripped corn oil was procured from TAMA Biochemical (Tokyo, Japan). UltraPower DNA/RNA safe dye was obtained from Gellex International (Tokyo, Japan). Bovine serum albumin fraction V, the Chelex 100 sodium form, 2'-deoxyguanosine monohydrate and monoclonal anti-β-actin antibodies (clone; AC-15) were obtained from Sigma-Aldrich (St Louis, MO). Anti-mouse IgG horseradish peroxidase (HRP)-linked antibody (#7074) and anti-rabbit IgG HRP-linked antibody (#7076) were obtained from Cell Signaling (Danvers, MA). The Midi Plus Ultrapure plasmid kit was obtained from Viogene (Taipei, Taiwan). The PlusGlow II, ChemilumiOne Super, ELISA POD substrate TMB kit and Protein Assay Bicinchoninate kits were obtained from Nakalai Tesque (Kyoto, Japan). The protease inhibitor cocktail was obtained from Roche Diagnostics (Indianapolis, IN). Anti-nitrotyrosine antibody (#06-284) was obtained from Upstate (Lake Placid, NY). 3,3,5,5,-Tetramethyl-1-pyrroline-*N*-oxide (M4PO) was from Labotec (Tokyo, Japan). The Immobilon-P transfer membrane was obtained from Millipore (Billerica, MA). The Can Get Signal immunoreaction enhancer solution was obtained from Toyobo (Osaka). The blocking reagent N101 was obtained from Nichiyu Life Sciences (Tokyo). Monoclonal antibodies against 4-hydroxy-2-nonenal (HNE)-modified proteins (clone; HNEJ-2),[15] 8-hydroxy-2'-deoxyguanosine (8-OHdG) (clone; N45.1)[16] and malondialdehyde (MDA)-modified proteins, and the highly sensitive ELISA kit for 8-OHdG were obtained from NIKKEN SEIL (Fukuroi, Japan). The anti-acrolein antibody (clone; 5F6)[17] was a kind gift from Koji Uchida, Nagoya University. Antibodies against cyclobutane pyrimidine dimers (CPDs) (clone; TDM-2) and 6-4 photoproducts (6-4 PPs) (clone; 64M-2) were used as previously described.[18] Hochest 33342 was obtained from Dojindo (Kumamoto, Japan). Polyclonal rabbit anti-mouse immunoglobulins/HRP (P0260) and Liquid DAB+ (K3468) were obtained from DAKO (Carpinteria, CA). The Histofine Simple Stain Rat Max-PO (mouse) was obtained from Nichirei (Tokyo, Japan). Alexa Fluora 488 Goat Anti-mouse IgG, ProLong Gold Antifade Reagent and Novex Chemiluminescent Substrates were obtained from Invitrogen (Carlsbad, CA). All other chemicals were of the highest quality available.

Animal experiments. The Animal Experiment Committee of the Nagoya University Graduate School of Medicine approved this experiment. Rats were housed in plastic cages in a temperature-controlled room (23–25°C with alternating 12-h light/12-h dark cycles) and were allowed free access to tap water and basal chow diet (Funahashi F-1, Chiba, Japan) during the experiment. F_1 hybrid rats were bred in-house by crossing female Fischer-344 and male Brown-Norway strains (Charles River, Yokohama, Japan).

Experimental setting of NEAPP. The same NEAPP device was used as previously described.[2,10] The electron density of this NEAPP is ~100 times higher than a conventional NEAPP. In this study, a quartz plate with a round window (diameter = 7 mm) was employed to adjust the irradiation area to match the well size of a standard clear flat bottom 96-well plate (Corning, Corning, NY). The distance from the bottom of the round window of the plasma head to the top surface of the 96-well plates was fixed at 10 mm. The flow rate of argon gas was set at 3 standard liter/min.

Detection of free radicals with electron spin resonance (ESR) spin-trapping. After a direct exposure of 300 mM M4PO (360 μl) in 96-well plates to NEAPP, samples were transferred to a disposable flat quartz cell (Radical Research, Tokyo, Japan). ESR signals were obtained with an FR-30 ESR Spectrometer (JEOL, Tokyo, Japan). Relative intensities of ESR spectra were calculated, using manganese as an internal standard signal.

Determination of conjugated dienes in linoleic acid and α-linolenic acid. Linoleic or α-linolenic acids were diluted to 1.5 mg/ml in chelex-treated ethanol. After exposure to NEAPP in plates at a volume of 360 μl, samples were transferred to UV-transparent cuvettes, and absorbance was measured at 234 nm using a spectrophotometer (GeneQuant 1300, GE Healthcare Life Sciences, Cambridge, UK). The formations of conjugated dienes were determined by the molar extinction coefficient (ε = 27,000/M cm).

Determination of TBARS in liposomes. Phosphatidylcholine (PC) and vitamin E-stripped corn oil were dispersed at a concentration of 16 mg/ml in chelex-treated milli-Q water, as previously described, with modifications.[19] Liposomes from Vitamin E-stripped corn oil were prepared with sonication for 5 min. The PC suspension was prepared with extensive vortexing. These samples were divided into 96-well clear bottom plates and treated with NEAPP. TBARS were measured according to the manufacturer's instructions. In brief, samples were incubated with a chromogenic reagent for 20 min at room temperature in 96-well black plates (Sumitomo Bakelite, Tokyo). The fluorometric assay was performed with PowerScan4 (DS Pharma Biomedical, Osaka). MDA was used as a standard.

Determination of the reduced form of glutathione (GSH) and TBARS in rat liver homogenates. Five 8-week-old F1 rats were euthanized. The liver was excised immediately and stored at −80°C. The liver was homogenized in 154 mM KCl (10%, w/v). Homogenates were centrifuged at 9,000 × *g*, and supernatants were harvested for the assays. After exposure to NEAPP, supernatants were used for determination of TBARS and GSH, and stored for western blot analysis. GSH levels were measured using DTNB as a chromogen.[20]

Detection of HNE-modified proteins, acrolein-modified proteins, MDA-modified proteins and 8-OHdG with immunohistochemistry in rat liver after NEAPP exposure *ex vivo*. For *ex vivo* studies, the liver was cut into ~5-mm fragements and placed on the well of flat bottom 96-well plates, which were covered with physiological saline to the top of the well. After NEAPP exposure, liver tissue was immediately fixed in 10% phosphate-buffered formalin overnight, followed by routine paraffin embedding, cutting and staining with hematoxylin and eosin for immunohistochemical analyses. Immunohistochemical analyses were performed as described.[20] Autoclaving in 10 mM citrate buffer, pH 6.0, at 121°C for 15 min was used for antigen retrieval. The primary antibodies used were against HNE-modified proteins (10 μg/ml), acrolein-modified proteins (2.5 μg/ml), MDA-modified proteins (1 μg/ml) and 8-OHdG (10 μg/ml). Alexa Fluora 488 Goat Anti-mouse IgG (20 μg/ml) was applied to slides with Hochest 33342 (1 μg/ml). After washing, slides were mounted with Prolong Gold Antifade Reagent. Fluorescent images were analyzed with a BZ-9000 (Keyence, Osaka).

Detection of double/single strand breaks and determination of 8-OHdG and photoproducts. Plasmid with an RNA I-Ready pSIREN-Retro-Q-ZsGreen vector backbone (6,632 bp) was used in this study.[21] To detect single/double strand breaks, plasmids were diluted to 2.78 ng/μl (1 μg/well in a volume of 360 μl) in chelex-treated water, then exposed to NEAPP. After concentrating the plasmids with 1-butanol, samples were applied to an agarose gel (0.8%, w/v) electrophoresis in TAE buffer (40 mM Tris, 20 mM acetate, 1 mM EDTA, pH 8.0). The signal intensities of bands were analyzed by ImageJ software (http://rsbweb.nih/gov/ij/). For the preparation of rat DNA, F1 rat liver was digested with proteinase K (200 μg/ml) in a digestion buffer (20 mM Tris-HCl pH 8.0, 400 mM NaCl, 5 mM EDTA, pH 8.0, 0.3% SDS (w/v)) at 37°C overnight. DNA was extracted with a standard procedure; 2'-deoxyguanosine (125 ng) and 2 μg of plasmid or rat genome DNA were placed in 96-well plates and treated with NEAPP. A competitive ELISA assay for 8-OHdG was performed according to the manufacturer's protocol.[16]

Detection of CPDs in tissue sections was performed as described.[18] Slides were incubated either with anti-CPDs antibody (TDM-2; 1:2,000) or anti-pyrimidine-pyrimidone (6-4) photoproduct antibody (64M-2; 1:1,000) after antigen retrieval with autoclaving in a 10 mM citrate buffer, pH 6.0, at 121°C for 15 min. Histofine Simple Stain rat Max-PO was applied and

doi: 10.3164/jcbn.14-40

visualized by liquid DAB+ as brown precipitates. To highlight the nuclear localization, nuclear counterstaining was omitted. ELISA for CPDs (10 ng DNA at 0.2 μg/ml for each well) was performed according to the manufacturer's protocol (ELISA POD substrate TMB kit).

Statistical analysis. Statistical analyses were performed using one-way analysis of variance (ANOVA) and an unpaired *t* test. The group of argon gas exposure was used as a control. Differences were considered significant when $p<0.05$. These analyses were performed with GraphPad Prism 5 Software (Graphpad Software, La Jolla, CA). The data are expressed as the mean ± SEM ($n = 3–6$) unless otherwise specified.

Results

ESR measurements. After direct exposure of a spin-trapping reagent, M4PO, to NEAPP, hydroxyl radicals were detected with ESR (Fig. 1A and B). Generation of hydroxyl radicals was time-dependent. We did not detect superoxide.

Increased conjugated dienes in linoleic acid and α-linolenic acid. After exposure to NEAPP, conjugated dienes were produced in linoleic and α-linolenic acids (Fig. 2A and B). NEAPP treatment up to 1 min did not significantly increase the oxidation of these polyunsaturated fatty acids.

Increased TBARS in PC and liposomes of vitamin E-stripped corn oil. After exposure to NEAPP, TBARS were elevated in PC and liposomes of vitamin E-stripped corn oil (Fig. 2C and D). NEAPP treatment significantly increased TBARS, starting 30 s in PC and 1 min in liposome of vitamin E-stripped corn oil in a time-dependent fashion.

NEAPP exposure of rat liver homogenate increased TBARS with no significant changes in GSH level. TBARS were significantly elevated after NEAPP treatment for 5 min. There were no alterations in GSH levels after NEAPP treatment up to 5 min (Fig. 3A and B).

Increase in HNE- and acrolein-modified proteins in rat liver after *ex vivo* NEAPP exposure. NEAPP exposure for 5 min induced a site-specific formation of HNE- and acrolein-modified proteins strongest at the surface toward the inside. However, this was not evident after NEAPP exposure for 30 s or 2 min (data not shown) or after 5 min of argon gas exposure (Fig. 3C, D, E and F). Of note was the fact that the immunostaining was single cell-dependent. A small amount of HNE-modified proteins were revealed in control specimens, but with diffuse staining. We detected neither MDA-modified proteins nor 3-nitrotyrosine using immunohistochemistry or western blot analysis (data not shown). We also evaluated the liver with hematoxylin and eosin staining, which revealed no significant changes even after exposure to NEAPP for 5 min (data not shown).

Formation of single/double DNA strand breaks and 8-OHdG. NEAPP induced strand breaks to the double-stranded plasmid DNA, which was demonstrated by the shift from a supercoiled form to open circular (single-strand break) or to linear (double-strand break) forms (Fig. 4A). Densitometric analysis revealed that single- and double-strand breaks after NEAPP irradiation occured in a time-dependent manner (Fig. 4B). Determination of 8-OHdG levels with ELISA demonstrated 8-OHdG formation from dG after NEAPP exposure. The amounts of 8-OHdG were the highest at 30 s and decreased in a time-dependent fashion thereafter (Fig. 4C). NEAPP treatment of plasmid and rat genomic DNA also induced 8-OHdG generation, which was also dependent on the exposure period (Fig. 4D and E).

Increased CPDs after NEAPP exposure. NEAPP exposure produced CPDs in the 5–7 most superficial hepatocyte cell layers with surface mesothelial cells whereas argon gas controls showed almost no immunostaining (Fig. 5A and B). Notably, we observed CPD- and 8-OHdG-double positive hepatocytes using serial sections (Fig. 5A and C). Determination of CPDs by ELISA

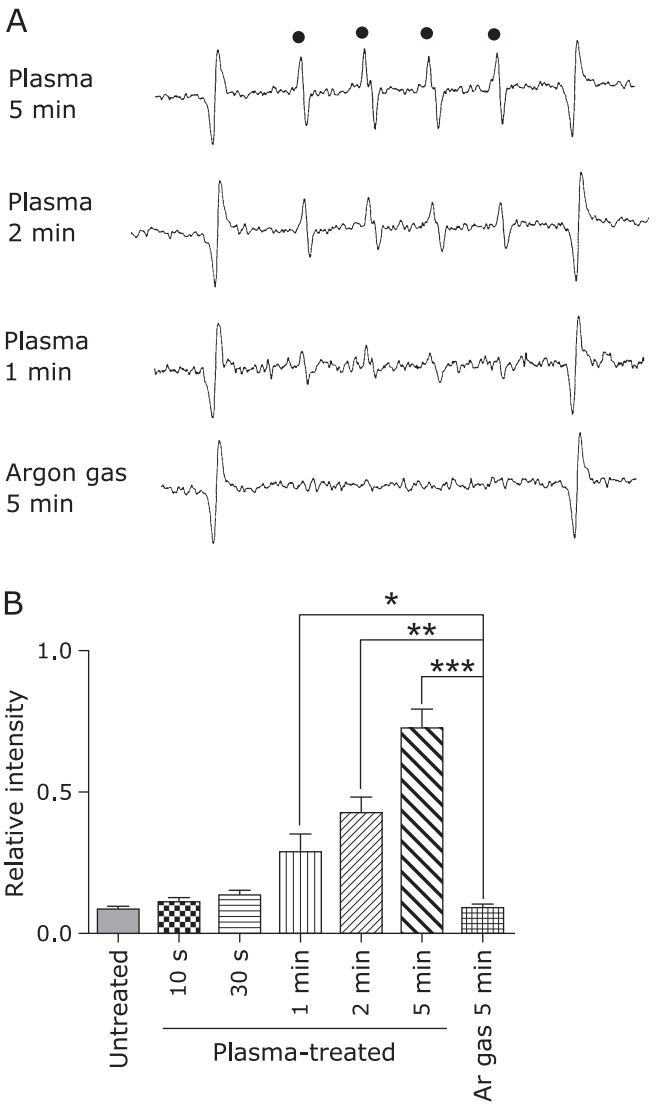

Fig. 1. Detection of hydroxyl radicals with ESR spin-trapping. (A) Representative images of ESR spectra with 3,3,5,5-tetramethy-1-pyrroline-*N*-oxide (M4PO) are shown. Manganese was used as an internal standard at both ends. (B) Exposure-dependent intensity were observed after NEAPP irradiation for 1, 2 and 5 min. Data are expressed as means ± SEM ($n = 3$; ANOVA, $p<0.0001$; *$p<0.05$, **$p<0.01$, ***$p<0.0001$ vs argon gas for 5 min).

demonstrated CPD formation after NEAPP exposure in both plasmid and rat genomic DNA (Fig. 5E and F). Whereas there was significant elevation of CPDs after 5 min in plasmids, there was significant elevation of CPDs after only 30 s of exposure in rat genomic DNA. We did not detect the formation of pyrimidine-pyrimidone (6-4) photoproducts (data not shown).

Discussion

There has been an enormous interest in applying novel engineering technology to clinical medicine. NEAPP is one such technique and is already used to disinfect skin wounds.[1] The next application could be in the treatment of advanced human cancers, such as peritoneal or pleural carcinomatosis, which often cannot be managed with currently available methods. Several promising studies have recently been reported.[9,11] However, fundamental information obtained via established methods about the molecular

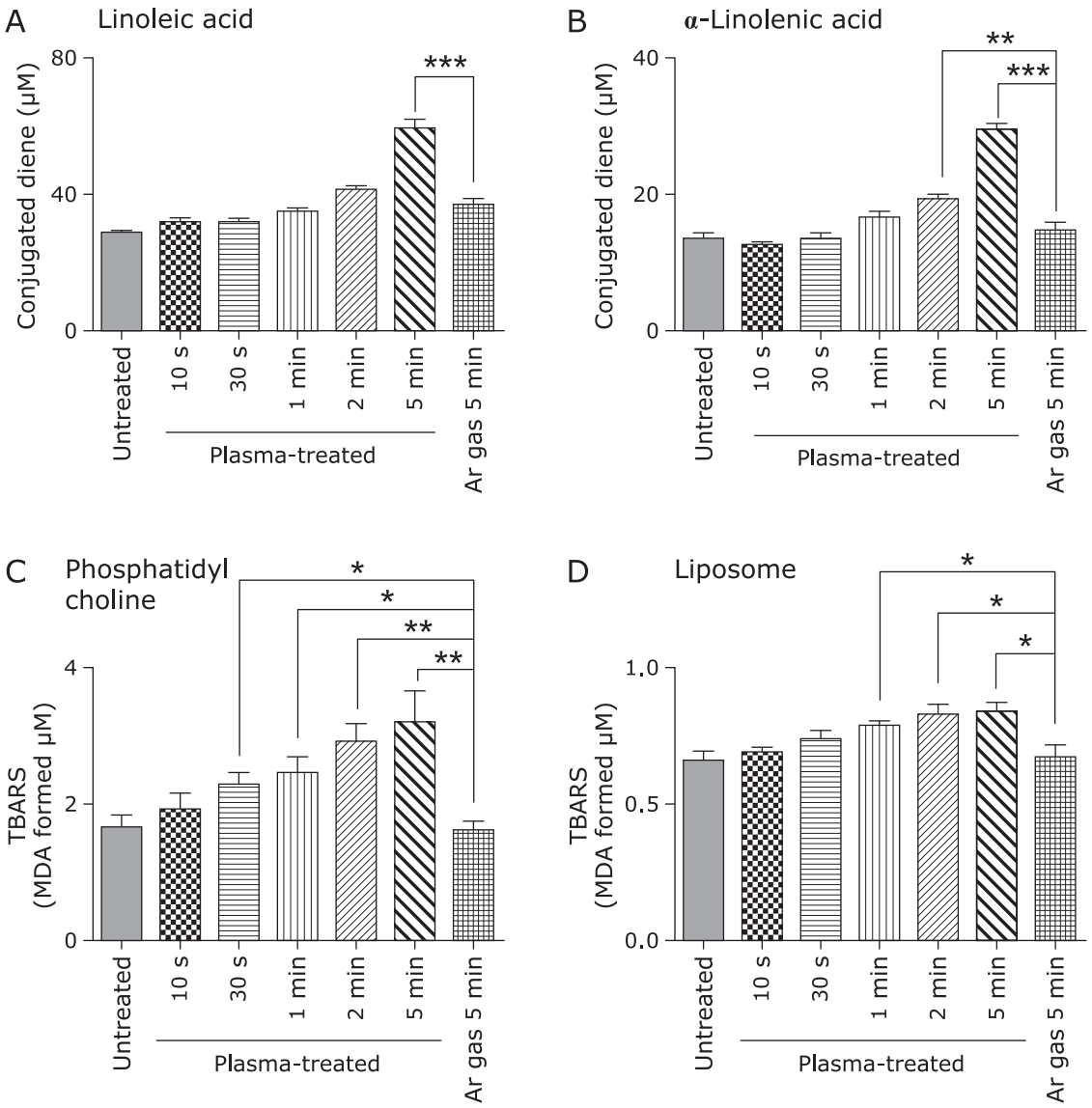

Fig. 2. Determination of conjugated diene in linoleic acid and α-linolenic acid, and TBARS in phosphatidylcholine (PC) and liposome of Vitamin E-stripped corn oil. (A) The formation of conjugated dienes in linoleic acid was significantly elevated after NEAPP irradiation for 5 min. (B) The formation of conjugated diene in α-linolenic acid was significantly elevated after NEAPP irradiation for 2 and 5 min. (C) TBARS in PC were significantly elevated after NEAPP irradiation for 30 s, 1, 2 and 5 min. (D) TBARS in liposomes of Vitamin E-stripped corn oil were also significantly elevated after NEAPP irradiation for 1, 2 and 5 min. Data are expressed as means ± SEM (n = 6 for conjugated diene assay; n = 5 for TBARS assay; ANOVA, p<0.0001, for A, B, p<0.001 for C, D; **p<0.01 and ***p<0.001 vs argon gas for 5 min).

effects of NEAPP has been lacking to date.

We found that hydroxyl radical is a major species with ESR spin-trapping technique (Fig. 1A and B). We observed that direct exposure of NEAPP modified lipids, proteins and nucleic acids with simultaneous but distinct ROS and UV reactions. Conjugated dienes are formed by the rearrangement of double bonds in polyunsaturated fatty acids. This reaction therefore consumes oxygen and yields lipid peroxide, which is subsequently broken down to release TBARS. Lipid peroxidation of linoleic acid, with two double bonds in a carbon framework, results in equimolar amounts of oxygen consumption, peroxide formation and conjugated diene formation.[22] In the cases of linolenic acid and phosphatidylcholine (PC), with three or more double bonds, the molar amounts of end products would be as follows: oxygen consumption>double bond break>peroxide>conjugated diene> TBARS.[22] Thus, conjugated dienes in linoleic acid are a sensitive method for detecting lipid peroxidation. Although we did not detect significant elevations in conjugated dienes after exposure to NEAPP for 30 s, 1 and 2 min (Fig. 2A), we detected an increase in TBARS as early as 30 s after exposure in PC and 1 min in liposomes (Fig. 2C and D), suggesting that TBARS is suited for this purpose. In our experimental model, we used NEAPP in the presence of atmospheric oxygen. Auto-oxidation of fatty acids during preparation might have elevated the background and masked any differences. Another possibility is the generation of singlet oxygen ($^1O_2$) from NEAPP. $^1O_2$ also reacts with unsaturated phospholipids to form lipid hydroperoxides, which add hydroperoxides at the 9', 10', 12' or 13' positions in linoleic acid.[23] Among the four isomers, only 9' and 13' peroxides can be measured in the conjugated diene form, suggesting that conjugated diene measurement detects half of the lipid peroxide that is generated by $^1O_2$.[23,24] $^1O_2$ formation has been reported using non-

doi: 10.3164/jcbn.14-40

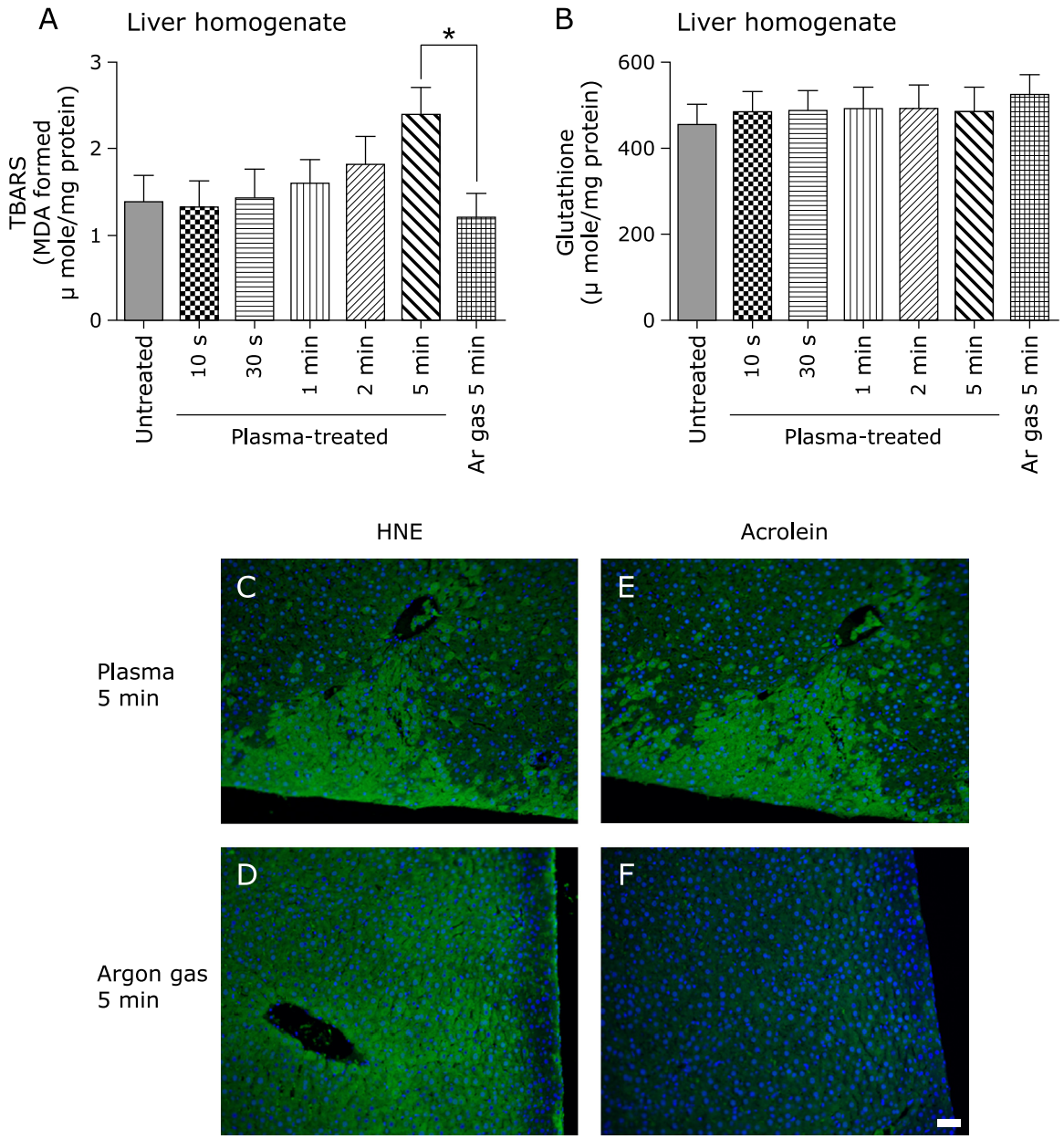

Fig. 3. Determination of TBARS and Glutathione reduced form (GSH) in rat liver homogenate and detection of HNE-modified proteins and acrolein-modified proteins by immunohistochemical analyses in rat liver. (A) TBARS in rat liver homogenates were significantly elevated after NEAPP irradiation for 5 min. (B) GSH in rat liver homogenate was unchanged after NEAPP treatment. Representative merged images of immunohistochemical staining for HNE-modified protein (C, D) and acrolein-modified proteins (E, F) are shown (scale bar, 50 μm). HNE and acrolein staining disclosed a depth-dependent spread in the hepatic parenchyma only after 5 min of NEAPP irradiation (C, E). There was no specific immunostaining in argon gas treated samples with a background diffuse staining in HNE-modified proteins (D, F). Data are expressed as means ± SEM (n = 5; *p<0.05 vs argon gas for 5 min).

thermal plasma.[25] Further studies are necessary to determine the more precise fraction of ROS in our device.

In a preliminary experiment, we used both liver and kidney for *ex vivo* exposure to NEAPP. We found that liver provides more consistent results. An advantage of rat liver is relative histological homogeneity with the presence of accumulated data on membrane phospholipids. PC and phosphatidylethanolamine are the major membrane phospholipids of liver, and PC has been reported to be composed of palmitic acid (~20%), stearic acid (~25%), oleic acid (~5%), linoleic acid (~10%), arachidonic acid (~30%) and docosahexaenoic acid (~10%).[26] We observed an increase in TBARS, but GSH did not decrease after liver homogenate exposure to NEAPP for 5 min (Fig. 3A and B). Thus far, we have studied a ferric nitrilotriacetate renal carcinogenesis model,[27–30] where Fenton reaction-mediated tissue damage and subsequent necrosis occur in the renal proximal tubules.[31] In this model, marked elevation of TBARS and a significant decrease in GSH were observed.[20] These data suggest that the oxidative stress associated with NEAPP is relatively mild.

Next, we evaluated protein modifications with oxidized lipid metabolites. We exposed bovine serum albumin or liver homogenates to NEAPP and subsequently performed western blots. We observed no differences between argon gas-treated and NEAPP-treated samples, using antibodies against HNE, MDA and

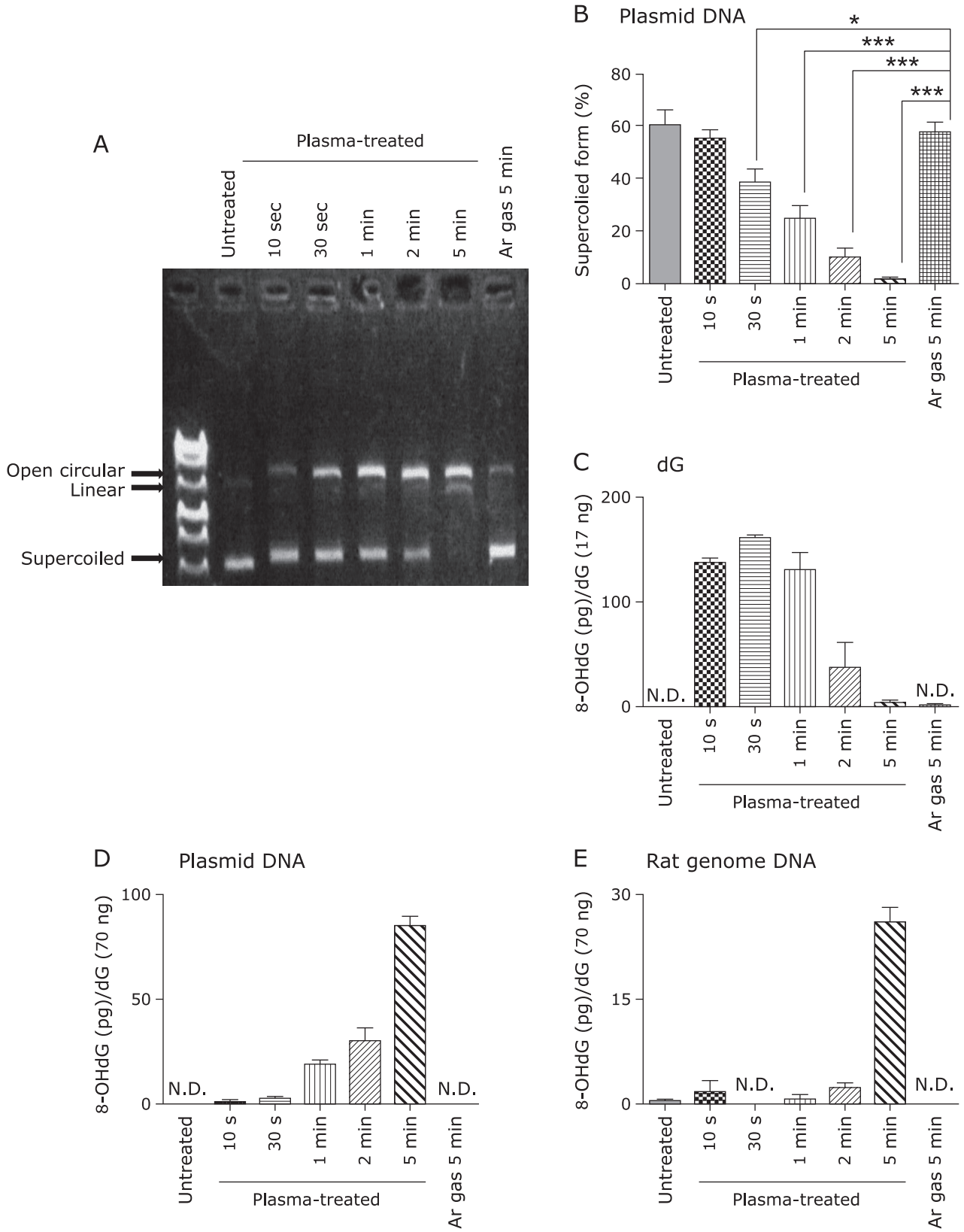

Fig. 4. Detection of single/double-strand breaks and determination of 8-OHdG. (A) Representative image of agarose (0.8%, w/v) electrophoresis is shown. NEAPP damaged double stranded plasmid DNA, as assessed by the shift from a supercoiled form to open circular and linear forms. (B) Densitometric analysis disclosed that single/double-strand breaks were observed in an NEAPP exposure time-dependent manner ($n = 6$). (C) 8-OHdG was formed from dG after NEAPP irradiation. The formation of 8-OHdG was highest at irradiation times of 30 s. (D) Irradiation of NEAPP increased the formation of 8-OHdG from plasmids in a time-dependent manner. (E) Irradiation of NEAPP increased the formation of 8-OHdG from rat DNA, also in a time-dependent manner. ELISA data (C)(D)(E) are demonstrated as means ± SEM ($n = 3$) and N.D. stands for not detectable and was less than 0.125 ng/ml or 6.25 pg/well (ANOVA, $p<0.0001$, for B–E; *$p<0.05$ and ***$p<0.001$ vs argon gas for 5 min).

doi: 10.3164/jcbn.14-40

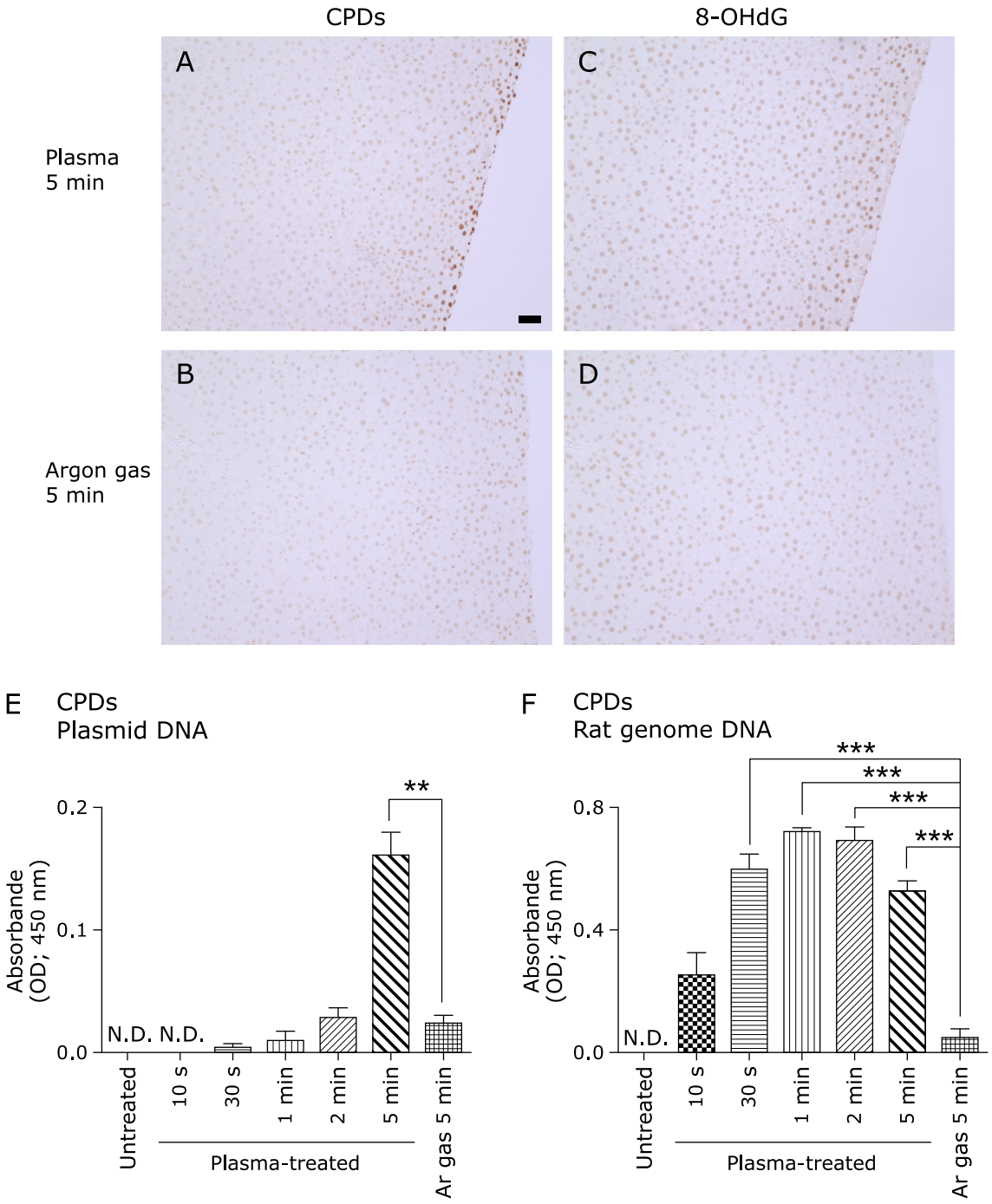

Fig. 5. Simultaneous immunohistochemical detection of cyclobutane pyrimidine dimers (CPDs) and 8-OHdG, with determination of CPDs with ELISA. Representative images of immunohistochemical staining for CPDs (A, B) (scale bar, 50 μm). (A) There are positive CPD signals in the nuclei of superficial hepatocytes as well as mesothelial cells. (B) There are almost no signals in the nuclei of hepatocytes. (C) This serial section after A shows the presence of 8-OHdG positive cells on the surface, indicating that those cells received dual damage from NEAPP. (D) Immunostaining of 8-OHdG was faint under the same experimental conditions. (E) CPDs were formed from plasmids after NEAPP irradiation in a time-dependent manner. (F) NEAPP exposure increased the formation of CPDs from rat genome DNA. The formation of CPDs was significantly increased after 30 s of irradiation (ANOVA, $p<0.0001$, for C, D; $^{**}p<0.01$ and $^{***}p<0.001$ vs argon gas for 5 min).

acrolein (data not shown). There was a significant difference in TBARS in the rat liver homogenate, but not on western blot analyses. We observed similar results when using a ferric nitrilotriacetate-induced model of renal injury in rodents, where western blot is less sensitive.[32–34] This is presumably due to the localization and the difference in the fraction of modified products between oxidized lipids and oxidized lipid (aldehydes)-modified proteins. To overcome this problem, we performed immunostaining of the exposed liver with various antibodies. We obtained a depth-dependent presence of HNE- or acrolein-modified proteins (Fig. 3C–F) and 8-OHdG (Fig. 5C) in hepatocytes after exposure to NEAPP for 5 min, confirming that superficial hepatocytes are oxidatively injured.

Modifications of DNA by NEAPP have recently attracted

interest.[3,4,25] Here, we observed single/double strand plasmid DNA breaks in a dose-dependent manner (Fig. 4A and B). We measured 8-OHdG formation with ELISA and found that the production efficiency was different in different systems: dG> plasmid>rat genomic DNA (Fig. 4C, D and E). Peak 8-OHdG formation was observed at 30 s in dG but at 5 min (with dose-dependency) in plasmid and rat genomic DNA. We suspect that 8-OHdG was further modified into a more oxidized form after NEAPP exposure of 1, 2 and 5 min, such as formamidopyrimidine-dG.[35] DNA damage releases MDA from sugar bases during the degradation via the Fenton reaction, which can be assessed as TBARS.[36] We thus measured TBARS in NEAPP-exposed dG. However, TBARS was not detected (data not shown, detection limit; 50 nM). This indicates that the reaction of NEAPP is essentially iron-independent.

CPDs specific for UV-induced damage were elevated after NEAPP exposure in plasmid and rat liver DNA (Fig. 5A, B, E and F). Whereas similar time-dependent elevations were observed for CPDs and peaked at 5 min for 8-OHdG in plasmids, CPDs formation had a much earlier peak (30 s) in rat genomic DNA. The differences in DNA sequences and three-dimensional conformations may have affected the peak timing of the two different kinds of DNA damage, but the simultaneous presence of 8-OHdG and CPD is certainly a unique situation that requires complex DNA repair and appears to be difficult to amend. DNA repair after NEAPP certainly needs more study, especially in cancer cells.

In conclusion, we collected fundamental data on the effects of direct NEAPP exposure on biological molecules including lipids, proteins and nucleic acids using our powerful NEAPP device and established methods in free radical biology. Our data suggest that the major effector molecule is the hydroxyl radical (or its equivalents), which works with UV irradiation within a few millimeters of depth in tissue. Therefore, NEAPP exposure of this kind could be controlled manually and may be usable for the eradication of surface cancer cells on the pleura and peritoneum.

Acknowledgments

This work was supported by Grant-in-Aid for Scientific Research on Innovative Areas (24108008; 24390094; 221S0001-04) from the Ministry of Education, Culture, Sports, Science and Technology of Japan, and partially supported by Grant-in-Aid for Young Scientists (B) (23790440 and 25860292) from the Japan Society for the Promotion of Science. We thank Mr. Nobuaki Misawa for his excellent preparation of tissue sections.

Abbreviations

ANOVA	analysis of variance
CPDs	cyclobutane pyrimidine dimers
DTNB	5,5'-dithio-*bis*-2-nitrobenzoic acid
ELISA	enzyme-linked immunosorbent assay
ESR	electron spin resonance
GSH	glutathione, reduced form
HNE	4-hydroxy-2-nonenal
HRP	horseradish peroxidase
M4PO	3,3,5,5-tetramethyl-1-pyrroline-*N*-oxide
MDA	malondialdehyde
NEAPP	non-equilibrium atmospheric pressure plasma
8-OHdG	8-hydroxy-2'-deoxyguanosine
$^1O_2$	singlet oxygen
6-4PPs	pyrimidine-pyrimidone (6-4) photoproducts
PC	phosphatidylcholine
ROS	reactive oxygen species
RNS	reactive nitrogen species
TBARS	2-thiobarbituric acid reactive substances
UV	ultraviolet

Conflict of Interest

No potential conflict of interest was disclosed.

References

1 Fridman G, Friedman G, Gutsol A, Shekhter A, Vasilets V, Fridman A. Applied Plasma Medicine. *Plasma Process Polym* 2008; **5**: 503–533.
2 Iseki S, Ohta T, Aomatsu A, *et al*. Rapid inactivation of *Penicillium digitatum* spores using high-density nonequilibrium atmospheric pressure plasma. *Appl Phys Lett* 2010; **96**: 153704.
3 Joshi SG, Cooper M, Yost A, *et al*. Nonthermal dielectric-barrier discharge plasma-induced inactivation involves oxidative DNA damage and membrane lipid peroxidation in *Escherichia coli*. *Antimicrob Agents Chemother* 2011; **55**: 1053–1062.
4 Brun P, Brun P, Vono M, *et al*. Disinfection of ocular cells and tissues by atmospheric-pressure cold plasma. *PLoS One* 2012; **7**: e33245.
5 Ahn HJ, Kim KI, Kim G, Moon E, Yang SS, Lee JS. Atmospheric-pressure plasma jet induces apoptosis involving mitochondria via generation of free radicals. *PLoS One* 2011; **6**: e28154.
6 Bundscherer L, Wende K, Ottmüller K, *et al*. Impact of non-thermal plasma treatment on MAPK signaling pathways of human immune cell lines. *Immunobiology* 2013; **218**: 1248–1255.
7 Schmidt A, Wende K, Bekeschus S, *et al*. Non-thermal plasma treatment is associated with changes in transcriptome of human epithelial skin cells. *Free Radic Res* 2013; **47**: 577–592.
8 Keidar M, Walk R, Shashurin A, *et al*. Cold plasma selectivity and the possibility of a paradigm shift in cancer therapy. *Br J Cancer* 2011; **105**: 1295–1301.
9 Tanaka H, Mizuno M, Ishikawa K, *et al*. Plasma-activated medium selectively kills glioblastoma brain tumor cells by down-regulating a survival signaling molecule, AKT kinase. *Plasma Med* 2011; **1**: 265–277.
10 Iseki S, Nakamura K, Hayashi M, *et al*. Selective killing of ovarian cancer cells through induction of apoptosis by nonequilibrium atmospheric pressure plasma. *Appl Phys Lett* 2012; **100**: 113702.
11 Utsumi F, Kajiyama H, Nakamura K, *et al*. Effect of indirect nonequilibrium atmospheric pressure plasma on anti-proliferative activity against chronic chemo-resistant ovarian cancer cells *in vitro* and *in vivo*. *PLoS One* 2013; **8**: e81576.
12 Matsumoto A, Takeishi S, Kanie T, *et al*. p57 is required for quiescence and maintenance of adult hematopoietic stem cells. *Cell Stem Cell* 2011; **9**: 262–271.
13 Ishimoto T, Nagano O, Yae T, *et al*. CD44 variant regulates redox status in cancer cells by stabilizing the xCT subunit of system xc(–) and thereby promotes tumor growth. *Cancer Cell* 2011; **19**: 387–400.
14 Kitano H. Cancer as a robust system: implications for anticancer therapy. *Nature Rev Cancer* 2004; **4**: 227–235.
15 Toyokuni S, Miyake N, Hiai H, *et al*. The monoclonal antibody specific for the 4-hydroxy-2-nonenal histidine adduct. *FEBS letters* 1995; **359**: 189–191.
16 Toyokuni S, Tanaka T, Hattori Y, *et al*. Quantitative immunohistochemical determination of 8-hydroxy-2'-deoxyguanosine by a monoclonal antibody N45.1: its application to ferric nitrilotriacetate-induced renal carcinogenesis model. *Lab Invest* 1997; **76**: 365–374.
17 Furuhata A, Ishii T, Kumazawa S, Yamada T, Nakayama T, Uchida K. Nε-(3-methylpyridinium)lysine, a major antigenic adduct generated in acrolein-modified protein. *J Biol Chem* 2003; **278**: 48658–48665.
18 Hattori Y, Nishigori C, Tanaka T, *et al*. 8-Hydroxy-2'-deoxyguanosine is increased in epidermal cells of hairless mice after chronic ultraviolet B exposure. *J Invest Dermatol* 1996; **107**: 733–737.
19 Hamazaki S, Okada S, Li JL, Toyokuni S, Midorikawa O. Oxygen reduction and lipid peroxidation by iron chelates with special reference to ferric nitrilotriacetate. *Arch Biochem Biophys* 1989; **272**: 10–17.
20 Okazaki Y, Kono I, Kuriki T, *et al*. Bovine lactoferrin ameliorates ferric nitrilotriacetate-induced renal oxidative damage in rats. *J Clin Biochem Nutr* 2012; **51**: 84–90.
21 Okazaki Y, Ma Y, Yeh M, *et al*. DMT1 (IRE) expression in intestinal and erythroid cells is regulated by peripheral benzodiazepine receptor-associated protein 7. *Am J Physiol Gastrointest Liver Physiol* 2012; **302**: G1180–G1190.

doi: 10.3164/jcbn.14-40

22 Yamamoto Y, Niki E, Kamiya Y, Shimasaki H. Oxidation of lipids. 7. Oxidation of phosphatidylcholines in homogeneous solution and in water dispersion. *Biochim Biophys Acta* 1984; **795**: 332–340.
23 Stratton SP, Liebler DC. Determination of singlet oxygen-specific versus radical-mediated lipid peroxidation in photosensitized oxidation of lipid bilayers: effect of beta-carotene and alpha-tocopherol. *Biochemistry* 1997; **36**: 12911–12920.
24 Terao J, Hirota M, Kawakatsu M, Matsushita S. Structural analysis of hydroperoxides formed by oxidation of phosphatidylcholine with singlet oxygen. *Lipids* 1981; **16**: 427–432.
25 Kalghatgi S, Kelly CM, Cerchar E, *et al*. Effects of non-thermal plasma on mammalian cells. *PLoS One* 2011; **6**: e16270.
26 Terao J, Asano I, Matsushita S. Preparation of hydroperoxy and hydroxy derivatives of rat liver phosphatidylcholine and phosphatidylethanolamine. *Lipids* 1985; **20**: 312–317.
27 Ebina Y, Okada S, Hamazaki S, Ogino F, Li JL, Midorikawa O. Nephrotoxicity and renal cell carcinoma after use of iron- and aluminum-nitrilotriacetate complexes in rats. *J Natl Cancer Inst* 1986; **76**: 107–113.
28 Okada S, Minamiyama Y, Hamazaki S, Toyokuni S, Sotomatsu A. Glutathione cycle dependency of ferric nitrilotriacetate-induced lipid peroxidation in mouse proximal renal tubules. *Arch Biochem Biophys* 1993; **301**: 138–142.
29 Toyokuni S. Molecular mechanisms of oxidative stress-induced carcinogenesis: from epidemiology to oxygenomics. *IUBMB Life* 2008; **60**: 441–447.
30 Akatsuka S, Yamashita Y, Ohara H, *et al*. Fenton reaction induced cancer in wild type rats recapitulates genomic alterations observed in human cancer. *PLoS One* 2012; **7**: e43403.
31 Hamazaki S, Okada S, Ebina Y, Midorikawa O. Acute renal failure and glucosuria induced by ferric nitrilotriacetate in rats. *Toxicol Appl Pharmacol* 1985; **77**: 267–274.
32 Hamazaki S, Okada S, Ebina Y, Li JL, Midorikawa O. Effect of dietary vitamin E on ferric nitrilotriacetate-induced nephrotoxicity in rats. *Toxicol Appl Pharmacol* 1988; **92**: 500–506.
33 Toyokuni S, Okada S, Hamazaki S, *et al*. Combined histochemical and biochemical analysis of sex hormone dependence of ferric nitrilotriacetate-induced renal lipid peroxidation in ddY mice. *Cancer Res* 1990; **50**: 5574–5580.
34 Uchida K, Fukuda A, Kawakishi S, Hiai H, Toyokuni S. A renal carcinogen ferric nitrilotriacetate mediates a temporary accumulation of aldehyde-modified proteins within cytosolic compartment of rat kidney. *Arch Biochem Biophys* 1995; **317**: 405–411.
35 Ober M, Müller H, Pieck C, Gierlich J, Carell T. Base pairing and repicatinve processing of the formamidopyridine-dG DNA lesion. *J Am Chem Soc* 2005; **127**: 18143–18149.
36 Iqbal M, Okazaki Y, Okada S. *In vitro* curcumin modulates ferric nitrilotriacetate (Fe-NTA) and hydrogen peroxide (H_2O_2)-induced peroxidation of microsomal membrane lipids and DNA damage. *Teratog Carcinog Mutagen* 2003; **Suppl 1**: 151–160.